

Prospective comparison of echocardiography versus cardiac magnetic resonance imaging in patients with Ebstein's anomaly

Christine H. Attenhofer Jost · Whitney D. Edmister · Paul R. Julsrud · Joseph A. Dearani · M. Savas Tepe · Carole A. Warnes · Christopher G. Scott · Nandan S. Anavekar · Naser M. Ammash · Heidi M. Connolly

Received: 6 August 2010 / Accepted: 14 July 2011 / Published online: 6 August 2011
© Springer Science+Business Media, B.V. 2011

Abstract Ebstein's anomaly (EA) is primarily diagnosed by echocardiography. The purpose of this study was to compare echocardiography and magnetic resonance imaging (MRI) in EA. Data from cardiac MRI and echocardiography were prospectively collected from 16 patients with EA. Imaging data also were compared with intraoperative findings. Information provided by MRI and echocardiography were comparable for left ventricular size and function, tricuspid valve reparability, qualitative assessment of right-sided cavities, and visibility of septal and anterior tricuspid valve leaflets. The posterior tricuspid valve leaflet and tricuspid valve fenestrations were

better visualized with MRI; associated heart defects were equally recognized, apart from small shunts that tended to be more readily diagnosed with echocardiography. Quantification of right-cavity size and right ventricular ejection fraction was possible only with cardiac MRI. The degree of tricuspid valve regurgitation was underestimated by echocardiography (2 patients) and by MRI (4 patients) when compared with intraoperative assessment. When evaluating EA, echocardiography and MRI provide complementary data. For visualization of the posterior tricuspid valve leaflet and quantitative assessment of right ventricular size and function, MRI is preferable. For appropriate risk stratification in EA, both MRI and echocardiography should be performed before cardiac surgery.

C. H. Attenhofer Jost
Cardiovascular Center Zurich, Zurich, Switzerland

W. D. Edmister · P. R. Julsrud · M. Savas Tepe
Department of Diagnostic Radiology, Mayo Clinic,
Rochester, MN, USA

J. A. Dearani
Division of Cardiovascular Surgery, Mayo Clinic,
Rochester, MN, USA

C. A. Warnes · N. S. Anavekar · N. M. Ammash ·
H. M. Connolly (✉)
Division of Cardiovascular Diseases, Mayo Clinic,
200 First St SW, Rochester, MN, USA
e-mail: connolly.heidi@mayo.edu

C. G. Scott
Division of Biomedical Statistics and Informatics,
Mayo Clinic, Rochester, MN, USA

Keywords Ebstein's anomaly · Echocardiography · Magnetic resonance imaging · Tricuspid valve

Abbreviations

BSA	Body surface area
EA	Ebstein's anomaly
LV	Left ventricle, left ventricular
LVIDd	Left ventricular internal dimension at end diastole
MRI	Magnetic resonance imaging
PWTd	Posterior wall thickness at end diastole
RV	Right ventricle, right ventricular
SWTd	Septal wall thickness at end diastole
TEE	Transesophageal echocardiography

Introduction

Ebstein's anomaly (EA) is rare and accounts for less than 1% of all congenital heart disease occurring in about 1 to 5 per 200,000 live births [1–4]. The typical diagnostic criteria include (1) adherence of the tricuspid valve leaflets to the underlying myocardium (failure of delamination); (2) downward (apical) displacement of the functional annulus (septal > posterior > anterior leaflet); (3) dilatation of the “atrialized” portion of the right ventricle (RV), with varying degrees of hypertrophy and thinning of the wall; (4) redundancy, fenestrations, and tethering of the anterior leaflet; and (5) dilatation of the right atrioventricular junction (true tricuspid annulus) [4–6]. The most typical feature of EA is apical displacement of the hinge point of the valve from the atrioventricular ring of more than .8 cm/m² body surface area (BSA).

Whereas the first case of EA was discovered during autopsy [7], this anomaly is now most commonly diagnosed with echocardiography [4, 8–11]. Magnetic resonance imaging (MRI) is used increasingly in the evaluation of patients with EA [12–17]. To our knowledge, echocardiography and MRI have not been compared directly when determining cardiac features of EA. The goal of the present study was to prospectively examine echocardiography and MRI data from patients with EA and to compare those results with operative findings in patients undergoing tricuspid valve surgery.

Methods

Study subjects

This study was approved by the Mayo Clinic Institutional Review Board. Sixteen patients prospectively underwent transthoracic echocardiography and clinically indicated MRI between January 7, 2003, and March 30, 2006. Findings from both examinations were compared for all 16 patients. Twelve patients underwent cardiac surgery after the 2 imaging procedures, and for those patients, imaging findings were compared with intraoperative findings.

Feature assessment

The following features were assessed with echocardiography and cardiac MRI: (1) morphology of all 3 tricuspid valve leaflets; (2) apical displacement; (3) feasibility of tricuspid valve repair on the basis of mobility of the leading edge; (4) regurgitation; (5) stenosis and leaflet fenestrations; and (6) size and function of the functional RV and the left ventricle (LV). Additional anomalies were also evaluated.

Echocardiography

Comprehensive, transthoracic, 2-dimensional and Doppler echocardiographic examinations were performed in all patients by use of the subcostal, parasternal, and apical windows. LV ejection fraction (biplane Simpson's method), LV muscle mass index ($[\text{LV mass} = .8 \times \{1.04[(\text{LVIDd} + \text{PWTd} + \text{SWTd})^3 - (\text{LVIDd})^3]\} + .6 \text{ g}]/\text{m}^2 \text{ BSA}$), and left atrial volume index (ellipsoid model) were measured according to the guidelines of the American Society of Echocardiography [18]. Diastolic function was assessed as previously described [19]. The systems used were the Acuson XP 256 or 512 (Acuson Corp, Mountain View, CA, USA) and the Hewlett-Packard Sonos 5000 (Hewlett-Packard Co, Palo Alto, CA, USA). Echocardiograms were digitally recorded. All echocardiographic examinations were reviewed by H.M.C. and C.H.A.J.

The displacement index was measured echocardiographically in the apical, 4-chamber view (Fig. 1a) as previously described [3]: in the echocardiographic image, the distance is measured from the point of insertion of the anterior mitral valve leaflet to the point of insertion of the septal tricuspid valve leaflet. RV volume and ejection fraction of the functional RV were assessed qualitatively but not quantitatively. The severity of RV dilatation and systolic dysfunction was assessed visually and categorized as normal, mild, moderate, or severe. Tricuspid valve regurgitation was assessed visually and categorized as none, mild, moderate, or severe. Additional findings (interatrial shunting, ventricular septal defect, normal or abnormal valve morphology, and left-sided heart anomalies) were noted if present.

The criteria used for LV noncompaction were previously published [20]. For the 12 patients who

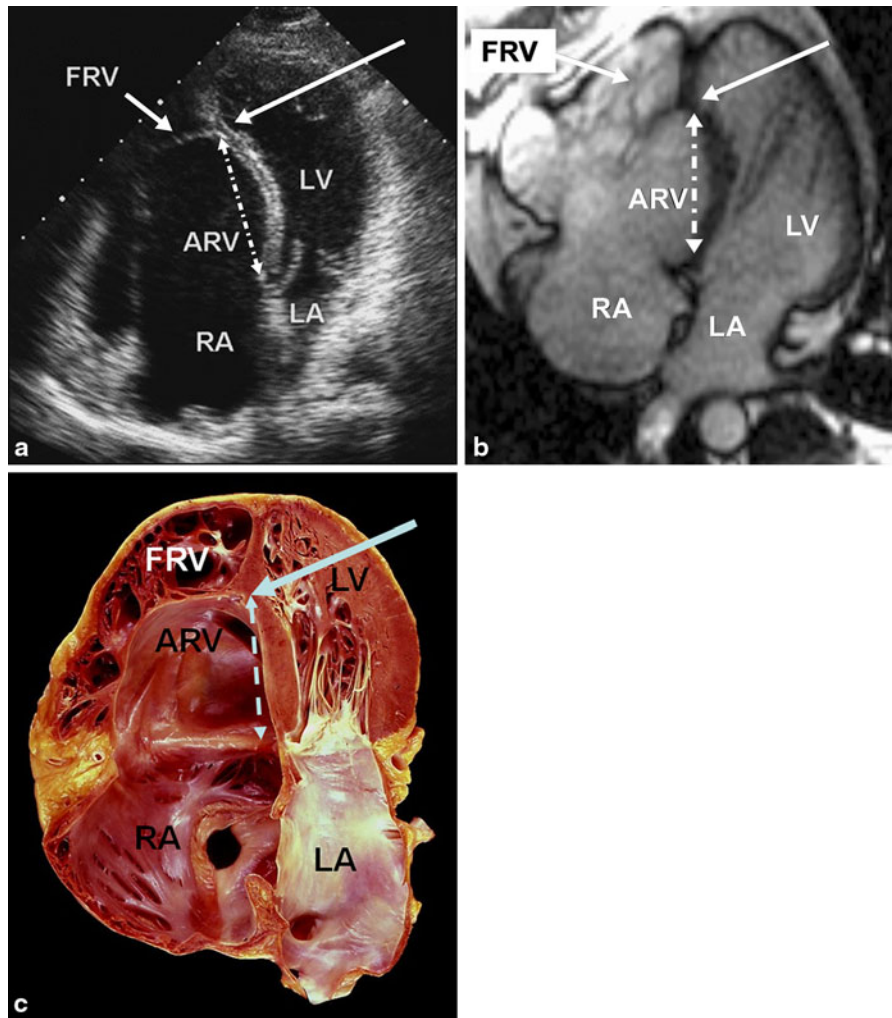


Fig. 1 Comparison of equivalent 4-chamber views and autopsy specimen of a heart with Ebstein's anomaly. **a** Echocardiogram. **b** Cardiac magnetic resonance image. **c** Autopsy specimen. Solid, *short arrows* point to the FRV. Solid, *long arrows* point to insertion of the apically displaced septal tricuspid valve leaflet. *Broken arrows* show the measurement

of displacement of the septal tricuspid leaflet. *ARV* atrialized right ventricle, *FRV* functional right ventricle, *LA* left atrium, *LV* left ventricle, *RA* right atrium. (Figure 1c courtesy of W. D. Edwards, MD, Mayo Clinic, Rochester, Minnesota. Used with permission.)

underwent cardiac surgery, intraoperative transesophageal echocardiography (TEE) was performed and the additional impact of this examination was reviewed. TEE was not performed in the 4 patients who did not undergo cardiac surgery.

Magnetic resonance imaging

MRI was performed with a 1.5-T system with cardiac gradients and phased-array cardiac coil (GE Healthcare, Piscataway, NJ, USA). Contrast-enhanced, magnetic

resonance angiography was not used for morphologic or functional assessment by MRI. The protocol for acquisition and analysis of MRI was determined before starting this study. The MRI protocol consisted of a 20-phase, electrocardiographically gated, breath-held, balanced, steady-state, free precession imaging sequence (8-mm slices with 2-mm skip) in the axial and short-axis planes through the atria and ventricles. Functional data were acquired by volumetric tracing contours in multiple planes to estimate end-systolic and end-diastolic volumes. In most cases, radial, balanced,

steady-state, free precession images were acquired along the right atrial–RV axis through the tricuspid valve to visualize all portions of the tricuspid valve in cross section. The morphology of all 3 tricuspid valve leaflets, tricuspid valvular stenosis and regurgitation, and leaflet fenestrations were assessed with the radial views when available. Apical displacement, feasibility of tricuspid valve repair on the basis of mobility of the leading edge, and size and function of the functional RV and LV were assessed with the axial and short-axis imaging planes. All MRI images were analyzed by P.R.J., M.S.T., and W.D.E.

LV, RV, right atrial, and atrialized RV volumes were estimated for each patient. LV function was best estimated in the short-axis planes, and RV function was best assessed in the axial planes. In most cases, radial, balanced, steady-state, free precession images were acquired along the right atrial–RV axis through the tricuspid valve to visualize all portions of the tricuspid valve in cross section. Reduction in RV ejection fraction was classified as follows: mild, 41–56%; moderate, 31–40%; or severe, 30% or less. RV volume indices of the residual trabeculated RV were classified as follows: normal, 66–126 mL/m² BSA for men and 50–118 mL/m² BSA for women; mildly dilated, 127–160 mL/m² BSA for men and 118–160 mL/m² BSA for women; moderately dilated, 161–200 mL/m² BSA for men and women; and severely dilated, greater than 200 mL/m² BSA for men and women [18, 21, 22]. The displacement index was measured from the mitral annulus to the insertion of the apically displaced septal tricuspid leaflet (Fig. 1b). Figure 1c shows a corresponding image from the autopsy of a 67-year-old man with severe EA. All MRI studies were performed after echocardiographic studies were complete, but images were interpreted by 3 radiologists who were masked to the results of the echocardiographic studies.

Surgery

Intraoperatively, the degree of tricuspid regurgitation and RV function was assessed by TEE; this information was also available to the surgeon. The 4-chamber view was most helpful. The surgeon examined the degree of delamination for each of the 3 leaflets, particularly the septal leaflet. Importantly, the areas of “failure of delamination” were analyzed, as were the points of tethering between the

true annulus and the apex of the RV. In addition, information about the status of the leading edge of the leaflet(s) and presence of linear attachments was reviewed. Other information obtained from TEE included the size of the true annulus and size and function of the functional and atrialized RV.

Gross inspection of the RV was performed after sternotomy and before the initiation of bypass. The surgeon specifically examined the acute margin of the RV and whether the anterior free wall of the RV collapsed during diastole. Findings that indicated poor RV function included loss of the acute margin and an anterior RV free wall that continuously bulged anteriorly during systole and diastole (concavity of the anterior wall during diastole was suggestive of better RV function). The inferior wall of the RV was also examined; it usually is markedly thinned in EA, especially in advanced cases. Poor RV function was indicated by dyskinesia in this area. Thinned, dyskinesic areas of the inferior RV wall typically were plicated during the course of operation. In general, the anterior RV free wall, particularly up in the area of the infundibulum, functioned the best and the inferior wall functioned the worst. Intraoperative assessment of tricuspid repair was performed with instillation of saline into the right ventricle with temporary pulmonary artery occlusion and then by post-bypass TEE imaging.

Statistics

Results are presented as mean (SD), and frequencies are expressed as a number (%) for dichotomous or qualitative variables. Contingency tables were analyzed for association using the χ^2 or Fisher exact test (where appropriate). Continuous variables were compared with the appropriate 2-sample test: a 2-sample *t* test when the variables met the assumptions of normal distribution and a Wilcoxon rank sum test otherwise. κ Statistics were used to describe and test agreement between different methods. The threshold for statistical significance was established at $P \leq .05$.

Results

Clinical characteristics of the 16 patients are shown in Table 1; 10 were female (63%). Three patients had undergone prior heart surgery, including atrial septal

Table 1 Clinical characteristics of the 16 patients

Patient	Sex	Age (years)	Prior cardiac intervention	Current heart surgery
1	F	53	No	TVR, 25-mm BP
2	M	54	Septal ablation of HOCM	No
3	M	47	No	TVR, 31-mm BP, BDCPA
4	F	47	No	TVR, 31-mm BP, VSD + ASD closure
5	F	17	Attempted TV repair + ASD closure EW	TVR, 33-mm BP
6	F	21	No	No
7	F	40	No	TVR, 33-mm BP, ASD closure, R Maze
8	M	22	No	TV repair
9	F	53	No	No
10	M	43	No	TV repair
11	M	56	No	TVR, 33-mm BP, ASD closure
12	F	52	No	TVR, 35-mm BP, ASD closure
13	M	53	No	TVR, 35-mm BP
14	F	36	ASD closure	TVR, 35-mm BP, ASD closure, R Maze
15	F	37	No	No
16	F	24	WPW ablation	TVR, 35-mm BP, ASD closure

ASD Atrial septal defect, BDCPA Bidirectional cavopulmonary anastomosis, BP Bioprosthesis, EW elsewhere, HOCM hypertrophic obstructive cardiomyopathy, R Maze right-sided Maze, TV tricuspid valve, TVR tricuspid valve replacement, VSD ventricular septal defect, WPW Wolff-Parkinson-White syndrome

defect closure (in 2 patients); 1 of these patients also had a previous unsuccessful attempt at tricuspid valve repair. The third patient had septal myectomy. All patients were in sinus rhythm during the examinations. Mean body weight was 74 [19] kg (range 45–108 kg); mean BSA was 1.85 (.20) m² (range 1.37–2.2 m²).

Comparison of findings from echocardiography versus MRI

The transthoracic echocardiographic image quality was good in 9 patients, moderate in 5, and poor in 2. The MRI quality was good in 14 patients, average in 1, and poor in 1.

Visibility of the tricuspid valve leaflets with transthoracic echocardiography and with MRI is shown in Table 2. The posterior leaflet was more difficult to visualize with transthoracic echocardiography and was identified in only 50% of patients. In an additional 2 patients (10 of 16 patients; 63%), it could be seen with TEE. By MRI, the posterior leaflet could be visualized in all patients (Fig. 2a). Displacement of the septal leaflet could be measured in all patients; although the displacement index was

Table 2 Comparison of tricuspid valve leaflet assessment and displacement index (N = 16)

Feature	Transthoracic echocardiography ^a	Magnetic resonance imaging
Leaflet visible		
Septal	16 (100%)	16 (100%)
Anterior	15 (94%)	16 (100%)
Posterior	8 (50%)	16 (100%)
Septal leaflet displacement		
Measurable	16 (100%)	16 (100%)
Overall, mm ^b	24 (8)	38 (18)
Index, mm/m ² BSA ^c	13 (5)	21 (10)
Tricuspid valve fenestrations ^d	4 (25%)	10 (63%)

BSA Body surface area

^a Continuous data are presented as mean (SD); categorical data as number of patients (%)

^b $P = .14$

^c $P = .15$

^d $P = .07$

greater with MRI, the difference between MRI and echocardiography measurements was not statistically significant ($P = .15$).

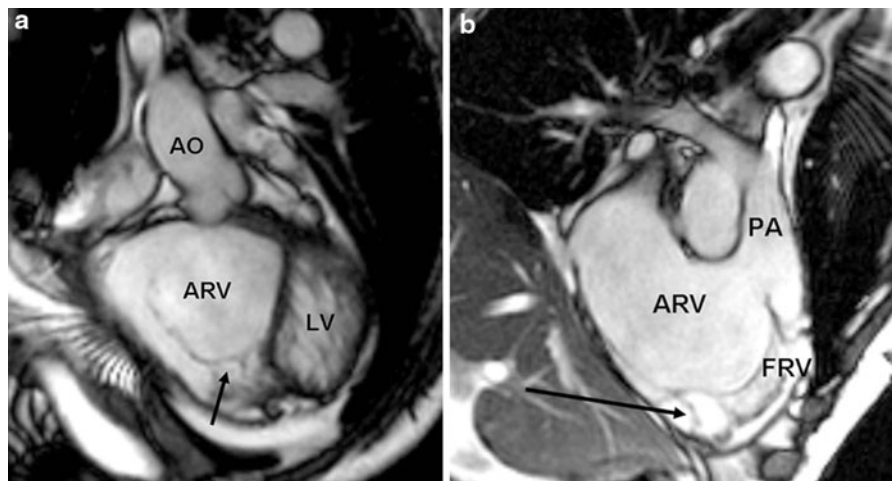


Fig. 2 Cardiac magnetic resonance images of a patient with Ebstein's anomaly. **a** Oblique transaxial image plane, which transects the ventricles (apex pointing inferiorly) and the great arteries superiorly. Exact delineation of the posterior leaflet (*arrow*). **b** Oblique sagittal image plane demonstrating the

inflow, apex, and outflow portions of the right ventricle. Example of tethering and adhesion of the anterior leaflet (*arrow*). *AO* aorta, *ARV* atrialized right ventricle, *FRV* functional right ventricle, *LV* left ventricle, *PA* pulmonary artery

A discrepancy was identified in the description of tricuspid valve fenestrations. Fenestrations were identified better with MRI than with echocardiography (Table 2). Adhesions and tethering of the anterior leaflet were well visualized with MRI (Fig. 2b).

Table 3 shows the comparison between RV ejection fraction and RV size assessed by echocardiography, MRI, and the intraoperative assessment by the surgeon. The values for RV size ($P = .92$) and function ($P = .91$) did not correlate significantly. Size of the atrialized RV, as measured by MRI, varied from 29 to 597 mL (average, 222 [139] mL). Size of the functional RV ranged from 35 to 300 mL (average, 133 [84] mL). Moderate or severe enlargement of the functional RV was indicated in 15 patients (94%) during the echocardiographic examination but in only 5 patients (31%) during MRI, reflecting the difficulty and discrepancy in assessing RV size. Therefore, the main difference was that by echocardiography and by assessment of the surgeon, the functional RV often appeared moderately to severely dilated but appeared normal by MRI.

RV ejection fraction could be quantitatively measured only by MRI; it ranged from 21 to 60% (average, 40% [12%]). Fractional area change is measured only rarely by echocardiography in patients with EA because of the difficulty in properly defining the borders of the functional RV. It could not be

Table 3 Comparison of RV function and volumes (N = 16)

Feature	Echocardiography	Magnetic resonance imaging	Surgery (n = 12)
Functional RV size, No. (%)			
Normal	1 (6)	9 (56)	0
Mild dilatation	0 (0)	2 (13)	0
Moderate dilatation	2 (13)	0 (0)	6 (50)
Severe dilatation	13 (81)	5 (31)	6 (50)
RV ejection fraction classification, No. (%)			
Normal	1 (6)	1 (6)	0
Mildly diminished	4 (25)	6 (38)	2 (17)
Moderately diminished	8 (50)	5 (31)	7 (58)
Severely diminished	3 (19)	4 (25)	3 (25)

RV Right ventricle

measured in any patient in the current study; the RV ejection fractions, measured by echocardiography (Table 3) were based on visual estimates.

LV size, mass, and morphology, as assessed by echocardiography and MRI, are shown in Table 4. Findings for LV ejection fraction and LV mass index were comparable between echocardiography and

Table 4 Comparison of additional findings for heart valves and LV size, mass, and function

Feature	Echocardiography	MRI	<i>P</i> values
LVEF, %	57 (9)	58 (10)	.42
LV mass index, g/m ² BSA	77 (52)	84 (30)	.08
Normal LV morphology	11 (69%)	15 (94%)	.30
Noncompaction	5 (32%)	1 (6%)	
Aneurysm of membranous septum	1 (6%)	0 (0%)	
Left atrial volume index, mL/m ² BSA	27 (13)	36 (19)	.04
Right atrial volume index, mL/m ² BSA	...	107 (74)	
Abnormal LV diastolic function	4 (25%)	...	
VSD	1 (6%)	0 (0%)	
ASD/PFO	10 (63%) ^a	6 (38%)	.09
Abnormal valve			
Aortic	2 (13%)	3 (19%)	.70
Mitral	3 (19%)	0 (0%)	
Pulmonary	1 (6%)	3 (19%)	.19

ASD Atrial septal defect, BSA body surface area, LV left ventricle, LVEF left ventricular ejection fraction, MRI magnetic resonance imaging, PFO patent foramen ovale, VSD ventricular septal defect

^a Transthoracic echocardiography, 7 patients; transesophageal echocardiography, 3 patients

MRI. LV morphology was described as abnormal more often with echocardiography: echocardiography showed 5 patients (31%) with noncompacted myocardium, whereas MRI showed only 1 patient (6%) with noncompaction. MRI (Fig. 3) shows the LV trabeculations slightly less clearly than echocardiography; however, the functional RV is clearly visualized.

A small aneurysm of the membranous septum and a small ventricular septal defect were missed by MRI. Abnormal diastolic function was observed in 4 patients with echocardiography. An interatrial communication was identified in 7 patients with transthoracic echocardiography and in 6 patients with cardiac MRI. In an additional 3 patients, an interatrial communication was found only with TEE. Intraoperative identification of

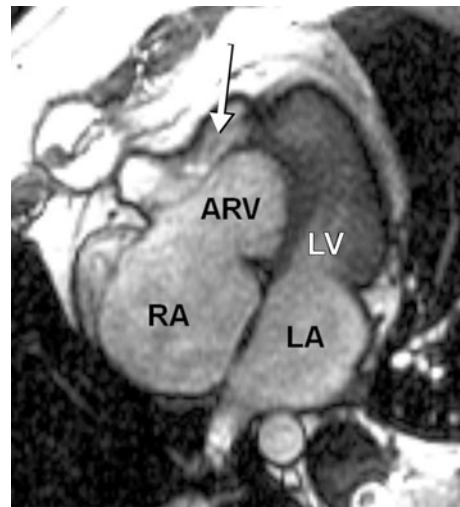


Fig. 3 Example of right and left ventricular assessment in Ebstein's anomaly by cardiac magnetic resonance imaging. This 4-chamber view of the heart is oriented with the apex pointing superiorly, corresponding to the image orientation of Fig. 1. The arrow indicates the functional right ventricle. ARV Atrialized right ventricle, LA left atrium, LV left ventricle, RA right atrium

interatrial shunting was consistent with the echocardiographic findings.

Intraoperative TEE was performed in all 12 patients undergoing surgery. Besides interatrial shunting, the following additional findings were observed with TEE but not with preoperative transthoracic echocardiography and MRI: cor triatriatum ($n = 1$); tricuspid valve fenestrations ($n = 1$); and hypoplastic pulmonary arteries ($n = 1$).

Qualitative assessment of the severity of tricuspid regurgitation, as determined by echocardiography and MRI, was compared with that estimated during surgery (Table 5). Compared with surgical estimates, tricuspid regurgitation was underestimated by echocardiography in 2 patients and underestimated in 4 patients by MRI. Overall, agreement between echocardiography (κ value .11; $P = .73$), cardiac MRI (κ value .18; $P = .49$), and the intraoperative assessment was not significant.

The assessment of reparability is summarized in Table 6. The MRI interpretation differed from the surgical findings in 3 of 12 patients (25%). The echocardiographic interpretation differed from the surgical findings in 2 patients (17%). In an additional 2 patients, reparability could be assessed only by TEE. In 1 patient, MRI findings suggested that the

Table 5 Comparison of assessment of degree of tricuspid regurgitation

Patient	Echocardiography	MRI	Surgeon ^a
1	Severe	Severe	Severe
2	Mild	Mild	...
3	Severe	Severe	Severe
4	Severe	Severe	Severe
5	Severe	Severe	Severe
6	Severe	Mild	...
7	Severe	Severe	Moderate
8	Severe	Severe	Severe
9	Moderate	Mild	...
10	Moderate	Moderate	Severe
11	Severe	Severe	Severe
12	Severe	Severe	Severe
13	Severe	Moderate	Severe
14	Moderate	Moderate	Severe
15	Moderate	Moderate	...
16	Severe	Moderate	Severe

MRI Magnetic resonance imaging

^a Four patients did not undergo surgery

valve was not repairable when surgical repair was actually performed. There was evidence for moderate agreement between echocardiography and the surgeon on reparability of the tricuspid valve (κ value .57; $P = .03$); however, MRI could not predict the surgeon's assessment of reparability (κ value .25; $P = .37$).

Table 6 Comparison of assessment of reparability in patients undergoing surgery (n = 12)

Patient	Echocardiography	MRI	Surgeon
1	Repair possible	Not repairable	Replacement, RRA
3	Repair possible	Not repairable	Replacement, RRA, bicaval PA
4	Not repairable	Not repairable	Replacement
5	Not repairable	Not repairable	Replacement, RRA
7	Not repairable (assessed by TEE)	Repair possible	Replacement
8	Repair possible	Not repairable	Repair, RRA
10	Repair possible	Repair possible	3-Leaflet repair, RRA
11	Not repairable	Repair possible	Replacement
12	Not repairable	Not repairable	Replacement, resection of inferior wall
13	Not repairable	Not repairable	Replacement
14	Not repairable (assessed by TEE)	Not repairable	Replacement
16	Not repairable	Not repairable	Replacement

MRI Magnetic resonance imaging, PA pulmonary anastomosis, RRA right reduction atrioplasty, TEE transesophageal echocardiography

Discussion

Combined assessment of EA by transthoracic echocardiography and cardiac MRI provided clinically valuable information. In this study, the findings from the 2 imaging methods were comparable in many respects (LV findings, tricuspid valve regurgitation and reparability, visualization of septal and anterior leaflet) and complementary in others (posterior leaflet and fenestrations were better visualized with MRI; small interatrial shunts or tiny ventricular septal defects may be more readily identified with echocardiography).

Importance of transthoracic echocardiography and TEE in EA

The importance of the echocardiographic assessment of all features of EA has been described previously [8, 10]. Tricuspid valve features that have been reported to correlate best to decreased functional capacity are absence of the septal leaflet and pronounced tethering, restriction of motion, and displacement of the anterior leaflet [10]. A comparison of 25 patients undergoing surgery showed excellent agreement between echocardiographic and surgical findings [23]. In that study, patients who had successful tricuspid valve repair differed from the group who needed tricuspid valve replacement in that the anterior leaflet was elongated—not tethered—and had a large excursion.

In the present study, the ejection fraction of the RV was assessed visually with echocardiography; quantitative assessment was not performed because it is difficult to trace the RV morphology in EA. Visual assessment of a normal LV has high interobserver variability, ranging up to 33%, but may still correlate quite well with assessment of ejection fraction by the Simpson or wall motion indices [24, 25]. Interobserver and intraobserver variability for the RV would likely be better using 3-dimensional echocardiography, which was not used in this series. Utility and excellent interobserver and intraobserver variability of real-time 3-dimensional echocardiography for RV quantification in congenital heart disease has been reported [26]. However, none of these patients with congenital heart disease had EA. In patients with EA, 3-dimensional echocardiography has been described as useful [27–29]. Our experience with 3-dimensional echocardiography in this patient population is limited. There are difficulties in consistently visualizing the thin tricuspid valve leaflets in patients with EA, especially in those with severe forms of EA. However, with technologic advances, 3-dimensional echocardiography will almost certainly provide invaluable incremental anatomic and functional information in the future.

Intraoperative TEE is important in the perioperative management of patients with congenital heart disease [30, 31]. In some of our patients, intraoperative TEE showed additional findings that led to a change in the operation. Interatrial shunting was identified in 3 additional patients; also, the assessment of leaflet anatomy, including assessment of reparability, was better with TEE in select patients. This suggests that routine use of intraoperative TEE should be compulsory for patients with congenital heart disease.

Importance of MRI in EA

MRI is a useful imaging technique in EA [12–14]. In 1974 and 1975, the Nobel-prize winning descriptions of the technology of MRI were made by P.C. Lauterbur, P. Mansfield, and R. Ernst [32]. As MRI of the heart continues to be developed for the purpose of assessing cardiac morphology and function, its usefulness in patients with congenital heart disease is becoming established [33]. One of the attractions of this imaging method is that the heart, great vessels,

and their anatomic relationships can be better delineated. More importantly, extracardiac anomalies are more reliably diagnosed, which can have important clinical implications when identified. This advantage stems from the fact that the images acquired using MRI are not limited by acoustic windows, as they are with traditional echocardiography; furthermore, the potential for a larger field of view allows a comprehensive, segmental, anatomic approach to the patient. In addition to cardiac structure, MRI has established value in assessment of cardiac function. The use of tailored MRI sequences allows for the assessment of wall motion, right and left ventricular ejection fraction, and, with newer technologies, blood flow [34, 35]. The value of cardiac MRI in the assessment of tricuspid regurgitation has been described previously [36]. Choi et al. [13] described the performance of the first series of MRI in EA in 9 patients. Axial images were more informative when visualizing the septal and anterior tricuspid valve leaflets. Coronal images were better for assessing the atrialized RV, the RV, and the posterior leaflet. Sagittal images seemed better for assessing the infundibulum and the pattern of attachment of the anterior leaflet. Small septal defects are difficult to reliably identify with cardiac MRI, given the decreased temporal resolution of the technique compared with traditional echocardiographic imaging [37]; this was also shown in our series. However, techniques for quantifying blood flow allow reliable estimation of shunt hemodynamics, which are important markers of the clinical significance of such lesions. A recent study has shown excellent performance of cardiac MRI in patients with ventricular septal defect and associated problems [38].

MRI offers several benefits during the preoperative evaluation of patients with EA. Accurate functional and volumetric data can be obtained for the right side of the heart. The ejection fraction can be quantitated for the functional RV and for the combined atrialized and functional portions of the RV. This accurately assesses both the current RV function and the expected RV function after tricuspid valve replacement or repair. Right atrial and RV volumes can be measured. In some cases, the atrial size was reduced by surgical resection of a portion of the atrial wall in EA.

Tricuspid valve leaflets in EA are often very thin—by cardiac MRI, they may not appear as sharply depicted as they are by echocardiography. However, visibility of the posterior leaflet is

increased and tricuspid regurgitation can be quantified by cardiac MRI [37]. Radial cine images along the axis of the RV allow visualization of the function and tethering of the anterior, posterior, and septal leaflets. The mitral leaflet was a good reference point for the correct position of the septal leaflet. The actual position of the base of the septal leaflet was reliably visualized by MRI in the axial plane.

Several studies have assessed RV function by using cardiac MRI [39, 40], but comparison with echocardiography has been limited [41, 42]. In our study, visual assessment of the RV function by echocardiography was comparable to quantitative assessment by MRI; however, the echocardiographic and surgical assessments of RV size differed from the MRI assessment. A possible explanation is that with visual assessment by the echocardiographer or the surgeon, the atrialized RV is included in the assessment, which is not done with MRI assessment; we realized this discrepancy only while analyzing this study. This emphasizes that for any imaging technique, the method must be exactly defined before the technique is compared with another technique.

Limitations of cardiac MRI include limited availability, problems in the presence of arrhythmias or claustrophobia, its lower temporal resolution compared with echocardiography, and less appreciation of valve motion and mobility compared with echocardiography.

Preoperative information and morphologic findings that affect clinical decision making

Tricuspid valve repair was performed infrequently in this small series (17%). This rate was considerably lower than usual for patients with EA at our institution—approximately 50% of our patients with EA undergo valve repair.

The prediction of tricuspid valve reparability was quite good with both methods (but not perfect). There was more agreement between echocardiography and the surgeon on reparability of the tricuspid valve (κ value .57; $P = .03$) than there was with MRI, which could not predict the surgeon's assessment of reparability as well (κ value .25; $P = .37$). To decide whether to repair or replace the tricuspid valve, the surgeon needs to know the degree of delamination of the anterior leaflet and the status of its leading edge. In general, for standard tricuspid valve repair, a large,

sail-like anterior leaflet with a very mobile edge is preferred because it facilitates coaptation with the ventricular septum or, in some cases, the abnormal septal leaflet [43–45]. Tethering or adherence of the leading edge of the anterior leaflet to the underlying endocardium precludes a satisfactory repair. In addition, information obtained through cardiac MRI or echocardiography is helpful when determining whether plication or resection of the atrialized RV is necessary. The finding in our study that the assessment of tricuspid valve reparability by cardiac MRI differed more often from the surgeon's assessment than it did with echocardiography might only be because echocardiographers had more experience knowing what the surgeon was specifically looking for. Thus, it is not a direct limitation of cardiac MRI technology.

The decision to proceed with operative intervention in patients with EA and the recommended operation must be tailored to individual patients. A comprehensive clinical assessment, transthoracic echocardiography, and MRI all provide important information used to determine the appropriate treatment plan for patients with EA. Patient symptoms and anatomic data are important when deciding the timing of intervention. Important anatomic and hemodynamic information that the cardiologist and surgeon need preoperatively includes (1) confirmation of the diagnosis, (2) assessment of RV and LV size and function, (3) determination of the reparability of the valve, and (4) identification of associated lesions that require operative attention. Intraoperative TEE findings can also help determine the best treatment plan. It is expected that 3-dimensional transthoracic echocardiography and TEE will expand the preoperative information gained by echocardiography and make this information more comparable to cardiac MRI. However, in our opinion, cardiac MRI should become and remain a compulsory preoperative screening method in any patient with EA undergoing surgery.

Limitations

Echocardiographic assessment of RV size and function and the degree of tricuspid regurgitation was made qualitatively in this study owing to ventricular and valve morphology. The lack of quantitative assessment by echocardiography limits a valid comparison of function and regurgitation parameters

between echocardiography and MRI, which is a major limitation of this study. Despite these limitations, qualitative assessment of ventricular size and function and the degree of regurgitation in patients with EA has been clinically useful.

Different classification schemes for EA have been used in the past; each nomenclature system has advantages and disadvantages [46, 47]. The extended Glasgow Outcome Scale assigns EA grades from 1 through 4 and describes the ratio of the volume of the combined right atrium and atrialized RV to that of the functional RV and LV at end-diastole, which might underestimate the role of the atrialized RV [47]. Although the grades have been related to outcome, classification schemes generally are imprecise as all patients with EA are different; our group did not use a classification scheme in this study, nor do we routinely use one in our clinical practice.

Our clinical experience with MRI in EA is still limited. This study was not designed to study the accuracy of diagnosing EA with MRI; rather, our goals were to compare the diagnostic techniques and to determine the strengths and weaknesses of each method. Additional experience will help to refine the reporting of anatomic findings from both echocardiography and MRI.

We acknowledge considerable selection bias in this study: the 16 patients were only a small fraction of patients with EA who were seen at our clinic during the study period. However, we included only patients who, according to the treating cardiologist, needed cardiac MRI. Nevertheless, this is still the largest study of EA patients comparing the 2 methods.

In our assessment in EA, we do not routinely perform saline-contrast echocardiography to search for interatrial shunting preoperatively because it can be identified intraoperatively by TEE or by the surgeon's visual inspection. Thus, the real accuracy of transthoracic echocardiography to diagnose interatrial shunts is underestimated.

Conclusions

For patients with EA, the data obtained with echocardiography and with cardiac MRI are complementary. Quantitative assessment of right-sided chamber size and function is best performed by MRI; however, identification of additional cardiac malformations,

valve anatomy, and reparability are better determined by echocardiography. Additional clinical experience with both techniques in all patients with EA is critical to facilitate appropriate comparison and to determine comparable reporting techniques, potential diagnostic pitfalls, and areas for improvement.

Conflict of interest None.

References

1. Perloff JK (2003) The clinical recognition of congenital heart disease, 5th edn. WB Saunders, Philadelphia, pp 194–215
2. Dearani JA, Danielson GK (2000) Congenital heart surgery nomenclature and database project: Ebstein's anomaly and tricuspid valve disease. *Ann Thorac Surg* 69(4 Suppl): S106–S117
3. Attenhofer Jost CH, Connolly HM, Edwards WD, Hayes D, Warnes CA, Danielson GK (2005) Ebstein's anomaly: review of a multifaceted congenital cardiac condition. *Swiss Med Wkly* 135(19–20):269–281
4. Attenhofer Jost CH, Connolly HM, Dearani JA, Edwards WD, Danielson GK (2007) Ebstein's anomaly. *Circulation* 115(2):277–285
5. Edwards WD (1993) Embryology and pathologic features of Ebstein's anomaly. *Progr Pediatr Cardiol* 2:5–15
6. Dearani JA, Danielson GK (2003) Ebstein's anomaly of the tricuspid valve. In: Mavroudis C, Backer CL (eds) *Pediatric cardiac surgery*, 3rd edn. Mosby, Philadelphia, pp 524–536
7. Mann RJ, Lie JT (1979) The life story of Wilhelm Ebstein (1836–1912) and his almost overlooked description of a congenital heart disease. *Mayo Clin Proc* 54(3):197–204
8. Oechslin E, Buchholz S, Jenni R (2000) Ebstein's anomaly in adults: Doppler-echocardiographic evaluation. *Thorac Cardiovasc Surg* 48(4):209–213
9. Patel V, Nanda NC, Rajdev S, Mehmood F, Velayudhan D, Vengala S et al (2005) Live/real time three-dimensional transthoracic echocardiographic assessment of Ebstein's anomaly. *Echocardiography* 22(10):847–854
10. Shiina A, Seward JB, Edwards WD, Hagler DJ, Tajik AJ (1984) Two-dimensional echocardiographic spectrum of Ebstein's anomaly: detailed anatomic assessment. *J Am Coll Cardiol* 3(2 Pt 1):356–370
11. Seward JB, Tajik AJ, Hagler DJ, Edwards WD (1984) Internal cardiac crux: two-dimensional echocardiography of normal and congenitally abnormal hearts. *Ultrasound Med Biol* 10(6):735–745
12. Eustace S, Kruskal JB, Hartnell GG (1994) Ebstein's anomaly presenting in adulthood: the role of cine magnetic resonance imaging in diagnosis. *Clin Radiol* 49(10):690–692
13. Choi YH, Park JH, Choe YH, Yoo SJ (1994) MR imaging of Ebstein's anomaly of the tricuspid valve. *AJR Am J Roentgenol* 163(3):539–543
14. Beerepoot JP, Woodard PK (2004) Case 71: Ebstein anomaly. *Radiology* 231(3):747–751
15. Didier D, Ratib O, Beghetti M, Oberhaensli I, Friedli B (1999) Morphologic and functional evaluation of

- congenital heart disease by magnetic resonance imaging. *J Magn Reson Imaging* 10(5):639–655
16. Chung T (2000) Assessment of cardiovascular anatomy in patients with congenital heart disease by magnetic resonance imaging. *Pediatr Cardiol* 21(1):18–26
 17. Cantinotti M, Bell A, Razavi R (2008) Role of magnetic resonance imaging in different ways of presentation of Ebstein's anomaly. *J Cardiovasc Med (Hagerstown)* 9(6):628–630
 18. Lang RM, Bierig M, Devereux RB, Flachskampf FA, Foster E, Pellikka PA et al. (2005) Chamber Quantification Writing Group; American Society of Echocardiography's Guidelines and Standards Committee; European Association of Echocardiography. Recommendations for chamber quantification: a report from the American Society of Echocardiography's Guidelines and Standards Committee and the Chamber Quantification Writing Group, developed in conjunction with the European Association of Echocardiography, a branch of the European Society of Cardiology. *J Am Soc Echocardiogr* 18(12):1440–1463
 19. Nagueh SF, Appleton CP, Gillebert TC, Marino PN, Oh JK, Smiseth OA et al (2009) Recommendations for the evaluation of left ventricular diastolic function by echocardiography. *J Am Soc Echocardiogr* 22(2):107–133
 20. Jenni R, Oechslin E, Schneider J, Attenhofer Jost C, Kaufmann PA (2001) Echocardiographic and pathoanatomical characteristics of isolated left ventricular non-compaction: a step towards classification as a distinct cardiomyopathy. *Heart* 86(6):666–671
 21. Maceira AM, Prasad SK, Khan M, Pennell DJ (2006) Reference right ventricular systolic and diastolic function normalized to age, gender and body surface area from steady-state free precession cardiovascular magnetic resonance. *Eur Heart J* 27(23):2879–2888 [Epub 2006 Nov 6]
 22. Alfakih K, Plein S, Thiele H, Jones T, Ridgway JP, Sivanathan MU (2003) Normal human left and right ventricular dimensions for MRI as assessed by turbo gradient echo and steady-state free precession imaging sequences. *J Magn Reson Imaging* 17(3):323–329
 23. Shiina A, Seward JB, Tajik AJ, Hagler DJ, Danielson GK (1983) Two-dimensional echocardiographic: surgical correlation in Ebstein's anomaly: preoperative determination of patients requiring tricuspid valve plication vs replacement. *Circulation* 68(3):534–544
 24. Gopal AS, Shen Z, Sapin PM, Keller AM, Schnellbaecher MJ, Leibowitz DW et al (1995) Assessment of cardiac function by three-dimensional echocardiography compared with conventional noninvasive methods. *Circulation* 92(4):842–853
 25. McGowan JH, Cleland JG (2003) Reliability of reporting left ventricular systolic function by echocardiography: a systematic review of 3 methods. *Am Heart J* 146(3):388–397
 26. van der Zwaan HB, Helbing WA, McGhie JS, Geleijnse ML, Luijnenburg SE, Roos-Hesselink JW et al (2010) Clinical value of real-time three-dimensional echocardiography for right ventricular quantification in congenital heart disease: validation with cardiac magnetic resonance imaging. *J Am Soc Echocardiogr* 23(2):134–140
 27. Vettukattil JJ, Bharucha T, Anderson RH (2007) Defining Ebstein's malformation using three-dimensional echocardiography. *Interact Cardiovasc Thorac Surg* 6(6):685–690 [Epub 2007 Sep 21]
 28. Pothineni KR, Duncan K, Yelamanchili P, Nanda NC, Patel V, Fan P et al (2007) Live/real time three-dimensional transthoracic echocardiographic assessment of tricuspid valve pathology: incremental value over the two-dimensional technique. *Echocardiography* 24(5):541–552
 29. Bharucha T, Anderson RH, Lim ZS, Vettukattil JJ (2010) Multiplanar review of three-dimensional echocardiography gives new insights into the morphology of Ebstein's malformation. *Cardiol Young* 20(1):49–53 [Epub 2010 Jan 19.]
 30. Hagler DJ, Tajik AJ, Seward JB, Schaff HV, Danielson GK, Puga FJ (1988) Intraoperative two-dimensional Doppler echocardiography: a preliminary study for congenital heart disease. *J Thorac Cardiovasc Surg* 95(3):516–522
 31. Ritter SB (1991) Transesophageal real-time echocardiography in infants and children with congenital heart disease. *J Am Coll Cardiol* 18(2):569–580
 32. Geva T (2006) Magnetic resonance imaging: historical perspective. *J Cardiovasc Magn Reson* 8(4):573–580
 33. Hawkes RC, Holland GN, Moore WS, Roebuck EJ, Worthington BS (1981) Nuclear magnetic resonance (NMR) tomography of the normal heart. *J Comput Assist Tomogr* 5(5):605–612
 34. Weber OM, Higgins CB (2006) MR evaluation of cardiovascular physiology in congenital heart disease: flow and function. *J Cardiovasc Magn Reson* 8(4):607–617
 35. Puranik R, Muthurangu V, Celermajer DS, Taylor AM (2010) Congenital heart disease and multi-modality imaging. *Heart Lung Circ* 19(3):133–144 [Epub 2010 Feb 23]
 36. Irwin RB, Luckie M, Khattar RS (2010) Tricuspid regurgitation: contemporary management of a neglected valvular lesion. *Postgrad Med J* 86(1021):648–655 [Epub 2010 Oct 18]
 37. Marcotte F, Poirier N, Pressacco J, Paquet E, Mercier LA, Dore A et al (2009) Evaluation of adult congenital heart disease by cardiac magnetic resonance imaging. *Congenit Heart Dis* 4(4):216–230
 38. Yoshimura N, Hori Y, Horii Y, Suzuki H, Hasegawa S, Takahashi M et al (2010) Comparison of magnetic resonance imaging with transthoracic echocardiography in the diagnosis of ventricular septal defect-associated coronary cusp prolapse. *J Magn Reson Imaging* 32(5):1099–1103
 39. Klein SS, Graham TP Jr, Lorenz CH (1998) Noninvasive delineation of normal right ventricular contractile motion with magnetic resonance imaging myocardial tagging. *Ann Biomed Eng* 26(5):756–763
 40. Sarkar D, Bull C, Yates R, Wright D, Cullen S, Gewillig M et al (1999) Comparison of long-term outcomes of atrial repair of simple transposition with implications for a late arterial switch strategy. *Circulation* 100(19 Suppl):III76–III81
 41. Papavassiliou DP, Parks WJ, Hopkins KL, Fyfe DA (1998) Three-dimensional echocardiographic measurement of right ventricular volume in children with congenital heart disease validated by magnetic resonance imaging. *J Am Soc Echocardiogr* 11(8):770–777
 42. Salehian O, Schwerzmann M, Merchant N, Webb GD, Siu SC, Therrien J (2004) Assessment of systemic right ventricular function in patients with transposition of the great arteries using the myocardial performance index: comparison with cardiac magnetic resonance imaging. *Circulation* 110(20):3229–3233 [Epub 2004 Nov 8]

43. Quinonez LG, Dearani JA, Puga FJ, O’Leary PW, Driscoll DJ, Connolly HM et al (2007) Results of the 1.5-ventricle repair for Ebstein anomaly and the failing right ventricle. *J Thorac Cardiovasc Surg* 133(15):1303–1310 [Epub 2007 Mar 26]
44. Dearani JA, O’Leary PW, Danielson GK (2006) Surgical treatment of Ebstein’s malformation: state of the art in 2006. *Cardiol Young* 16(Suppl 3):12–20
45. Brown ML, Dearani JA, Danielson GK, Cetta F, Connolly HM, Warnes CA et al (2008) Mayo clinic congenital heart center. The outcomes of operations for 539 patients with Ebstein anomaly. *J Thorac Cardiovasc Surg* 135(5): 1120–1136 (1136.e1-7)
46. Carpentier A, Chauvaud S, Mace L, Relland J, Mihaileanu S, Marino JP et al (1988) A new reconstructive operation for Ebstein’s anomaly of the tricuspid valve. *J Thorac Cardiovasc Surg* 96(1):92–101
47. Celermajer DS, Bull C, Till JA, Cullen S, Vassilikos VP, Sullivan ID et al (1994) Ebstein’s anomaly: presentation and outcome from fetus to adult. *J Am Coll Cardiol* 23(1): 170–176